

CONFERENCES AND SYMPOSIA

PACS numbers: 92.60.Pw, **93.85.–q**

Physics of lightning: new model approaches and prospects for satellite observations

D I Iudin, S S Davydenko, V M Gotlib, M S Dolgonosov, L M Zelenyi

DOI: https://doi.org/10.3367/UFNe.2017.04.038221

Contents

Abstract. **Fundamental problems of lightning physics are reviewed, and recent advances in the instrumental (primarily satellite) detection of atmospheric discharge phenomena are discussed. The formation of plasma spots with the parameters necessary for the initiation and development of a lightning discharge in a thundercloud is regarded as a nonequilibrium phase transition induced by electrostatic noise. The noise is caused by the collective dynamics of charged hydrometeors, i.e., ice particles and water drops suspended in a convective flow. The interaction of plasma formations and their polarization in a large-scale intracloud electric field ensure the efficient generation of streamers, whose description in terms of random graphs and percolation theory forms the basis for the phenomenological representation of discharge as a fractal dissipative structure. This approach enables solving a number of key problems surrounding thunderstorm electricity, including the lightning initiation mechanism in essentially subthreshold electric fields, the properties and morphology of various types of lightning discharges, and a self-consistent description of the broadband electromagnetic radiation they emit. Prospects for the further development of the model are discussed and the role of forthcoming satellite experiments in the observation of intense electromagnetic radiation from thunderstorm clouds is examined.**

D I Iudin Institute of Applied Physics, Russian Academy of Sciences, ul. Ul'yanova 46, 603950 Nizhny Novgorod, Russian Federation
E-mail: iudin@ipfran.ru
S S Davydenko Space Research Institute, Russian Academy of Sciences, ul. Profsoyuznaya 84/32, 117997 Moscow, Russian Federation; Institute of Applied Physics, Russian Academy of Sciences, ul. Ul'yanova 46, 603950 Nizhny Novgorod, Russian Federation
E-mail: davyd@ipfran.ru
V M Gotlib, L M Zelenyi Space Research Institute, Russian Academy of Sciences, ul. Profsoyuznaya 84/32, 117997 Moscow, Russian Federation
E-mail: gotlib@iki.rssi.ru, zelenyi@iki.rssi.ru
M S Dolgonosov National Research University 'Higher School of Economics', ul. Myasnitskaya 20, 101000 Moscow, Russian Federation; Space Research Institute, Russian Academy of Sciences, ul. Profsoyuznaya 84/32, 117997 Moscow, Russian Federation
E-mail: cactus@iki.rssi.ru

Received 30 September 2017
Uspekhi Fizicheskikh Nauk **188** (8) 850 – 864 (2018)
DOI: https://doi.org/10.3367/UFNr.2017.04.038221
Translated by A L Chekhov; edited by A M Semikhatov

Keywords: atmospheric electricity, physics of lightning, satellite observations of lightning discharges

1. Question of lightning initiation and evolution and new observation possibilities

Lightning is a spark electric discharge that can be observed in planet atmospheres during thunderstorms, volcano eruptions, and dust storms. The annual global average rate of lightning flashes is several dozen discharges per second [1]. The main mechanism of lightning activity is the transformation of atmospheric mass mechanical motion into electric energy [2]. Lightning has ben registered on Jupiter and its satellite Io and on Venice, Uranus, and Saturn in the optical, radio, and gamma ranges by spacecraft with flyby and orbital trajectories, as well as by those with descent modules (see, e.g., [3–7]).

Although lightning is one of the most conspicuous atmospheric phenomena, the understanding of its formation mechanisms, even in Earth's atmosphere, remains at a regrettably low level. Despite significant theoretical efforts and broad experimental data on natural and laboratory discharges [2, 8], self-consistent physical models for lightning discharges have not yet been developed due to the complexity of the research object. An explanation of spark channel formation (and hence the generation of a spark discharge) is currently given in the framework of the streamer theory for electrical breakdown in gases. According to this theory, electron avalanches, which form in the electric field of a discharge gap, under specific conditions give rise to streamers — dimly glowing thin forked channels containing ionized gas atoms and free knocked-out electrons. Interaction among the streamers leads to the formation of a so-called leader — a weakly glowing discharge that paves the way for the main discharge. In propagating from one electrode to another, the leader covers the discharge gap and links the electrodes with a continuous conducting channel. After that, the main discharge follows the formed path in the opposite direction with a sharp increase in the current and released energy. The channel rapidly expands, forming a shock wave on its boundaries.

Over recent years, there has been significant progress in describing certain aspects of discharge, particularly single steamer discharge [9] and hot plasma dynamics in the leader channel [10]. However, key problems regarding the description of the electric discharges in the cloud environment remain unsolved. These problems include the physical mechanisms of the discharge initiation in a subthreshold electric field, asymmetry in the dynamics and properties (including the propagation character) of positive and negative leaders, the streamer–leader transition mechanism, the leader channel conductivity dynamics, and many others. At the same time, despite theoretical disagreements, there is a developed common description of lightning discharge initiation, which includes three steps [11, 12]:

(1) an increase in large-scale electric fields in a cloud due to convective and microphysical processes;

(2) the appearance of local regions of a strong electric field with increased background ionization, which provides the generation and propagation of streamers;

(3) the flow of an electric current through the strong field regions with enough power to create a fully ionized channel of a lightning leader.

In describing the first stage of lightning evolution, it is important to take into account that planet atmospheres are a weakly conducting plasma with a moderate ionization level supported by galactic and solar cosmic rays, the Sun's ultraviolet radiation, high-energy particles from planet magnetospheres, and radionuclide emanations. The physical possibility of charge separation and accumulation of electrical energy stems from the fact that the collision rate of charge carriers with neutral molecules in the atmosphere is much lower than their plasma frequency. In other words, the relaxation time of the accumulated charge is much longer than the plasma oscillation period.

It is also important that the relaxation time is longer than the characteristic time scales of the corresponding aerodynamic and thermodynamic processes that determine the large-scale evolution of the electric field in the atmosphere. Moreover, for such a relation between the plasma frequency and the collision rate, the Debye radius is very large compared with the mean free path of the charges and is therefore no longer a spatial scale of plasma quasi-neutrality. As a result, the charged components are captured by the neutral medium motion and take part in large-scale charge separation in the presence of particles suspended in the atmospheric flow (ice particles, water drops (hydrometeors), grains of sand, dust particles, and aerosols) and through the corresponding mechanisms (charge separation due to particle collisions, ion capture, thermodynamic phase transitions, etc.).

The presence of moving particles is the main difference between the cloud environment and the normal gaseous atmosphere and plays a major role in the initiation of a lightning discharge. In electrodynamic, hydrodynamic, and plasmachemical processes of microscopic charge separation, cloud particles lose and acquire electrons, which leads to the formation of oppositely charged cloud particles. Usually, the positively charged particles are much lighter than the negatively charged ones. Therefore, the convection in the cloud leads to large-scale charge separation, i.e., to the formation of charged layers and the generation of a large-scale electric field.

For an electric discharge to be generated in a cloud, the corresponding field has to be stronger than the electric strength of the atmospheric air. Electric strength (or breakdown field) $E_{\rm b}$ of the medium is defined by the equilibrium between the processes of free electron creation and disappearance. In the absence of inhomogeneities, this equilibrium condition is determined by the threshold for the electron number exponential growth and amounts to the equality between the ionization rate $v_{\rm i}$ and the rate of electron attachment to oxygen atoms in the air $v_{\rm a}$ as a function of the applied field [8]. This is because the elementary charge attachment to the electronegative component of the air, oxygen, plays the main role in the mechanisms of free electron disappearance. Under normal conditions in dry air, the electron lifetime is only 10 ns [8]. The attachment leads to the formation of negative oxygen ions, which have a very low mobility and slow down the charge development. The air breakdown field is in the range $E_{\rm b} \approx 2.6 - 3.2$ MV m^{-1} under normal conditions at sea level and decreases with height proportionally to the atmospheric pressure. In a subthreshold electric field, the electron attachment rate in air is higher than the ionization rate. However, multiple balloon measurements show that the electric field amplitude in a thundercloud is one order of magnitude less than the threshold value needed for normal electric breakdown in air [2].

This means that the second stage of the evolution of lightning assumes the existence of a mechanism for the amplification of relatively weak macroscopic fields of the thundercloud, so as to initiate and support the evolution of streamers. The possibility of lightning discharge initiation in strongly subthreshold electric fields is currently the main intrigue in lightning physics.

To explain the lightning discharge initiation scenario, or at least its second stage, several theories have been introduced at different times. Among them, the most popular ones are lightning generation through the initiation of a positive streamer from a hydrometeor surface [13–15] and lightning evolution as a breakdown through runaway electrons [16–18]. Later, it was shown in [19–21] that a runaway electron avalanche does not lead to an electric breakdown due to the transverse spreading of the avalanche and corresponding decrease in the concentration of the generated plasma. The authors of [19, 20] also believe that such diffusive discharges cannot result in the formation of a lightning leader. Therefore, the authors of [19] suggested a breakdown scheme based on runaway electrons, in which the background cosmic rays induce a significant inhomogeneity of the electric field resulting in the acceleration of positrons created during the discharge. This actually establishes positive feedback and significantly increases the runaway electron flow. The created burst of the electric field close to the discharge boundary under pressure at sea level can exceed 1 MV m^{-1} and thus support the traditional discharge process.

Besides considering positron influence on the runaway electron breakdown evolution, a hybrid mechanism was suggested in [11] to explain the local field enhancement. This mechanism links the runaway electron breakdown with the initiation of positive streamers from the hydrometeor surface. According to [11], the initiation of the lightning channel occurs similarly to the spatial streamer formation (negative leader steps) under laboratory conditions. In fact, paper [11] has closed the loop in the search for the lightning initiation mechanism: the scientific community working on thunderstorm electricity problems returned to the idea of a traditional breakdown that develops as a positive streamer system from the hydrometeor surface.

Later, a more thorough theoretical investigation of positive streamer initiation using the hydrometeor model was performed in [22]. It was shown that the traditional breakdown can be initiated in the electric field of half the strength of the air electric strength. Soon, the modeling results for streamer formation were presented in [9] for electric fields of at least one third the strength of the breakdown threshold. According to [9], the excitation of a stable streamer from a model hydrometeor in a subthreshold field of only $0.3E_{\mathrm{b}}$ is possible only under the condition of an increased preionization level of the medium in front of the developing streamer. As a possible source of the increased preionization level, the authors of [9] emphasize the corona discharge development, which is caused by the convergence of charged and external-field polarized hydrometeors [23, 24].

In [25], the author considers metastable nitrogen and oxygen molecules as a possible source of the increased ionization level and for the first time raises the question of the role of electron detachment in the lightning initiation process. It is known that the detachment effects — electron escape from negative ions — play an important role in stationary discharges and compensate the attachment effect. These processes decrease the electron loss and, as experiments on glow discharges in electronegative gases show, their effect can be quite significant [8]. If the electron population losses were not so strong, then, according to [25], the detachment compensating effect would be significantly pronounced inside the thundercloud, and the breakdown field E_{b} would be reduced several-fold.

The above-described main mechanisms of the formation of local regions with a high electric field have both advantages and disadvantages. Even under the assumption that the thundercloud electric field can be locally enhanced due to the breakdown on runaway electrons and/or positive streamer system formation (or due to another mechanism), there is still a problem connected with the third and final stage of the lightning initiation scenario: how can the existence of a high electric field in compact regions of the intracloud space provide the development of the hot leader stage of the lightning discharge? The transition from the discussion of specific local field enhancement mechanisms to the lightning leader system formation is usually made in the literature by referring to 'conventional' and 'common' breakdown mechanisms, which are not clearly defined. This means that the problem of the transition to the lightning leader stage not only remains unsolved but also lacks a proper description [11].

The problems connected with lightning initiation became particularly complicated in the 1980s after the discovery of compact intracloud discharges — the most powerful natural sources of high-frequency radiation in Earth's atmosphere (see Section 3.3). On the one hand, compact intracloud discharges (CIDs) have a number of unique properties. In particular, CIDs result in a short superpower burst of electromagnetic radiation in the very high frequency (VHF) range and an intensive short bipolar pulse of the electric field, similar to the pulse generated during the return stroke of a typical cloud–ground discharge. On the other hand, several authors noted an analogy between CIDs and initial breakdown pulses (IBPs), which led to attempts to describe these phenomena using the same approach. This resulted in an even greater discrepancy between the concept of lightning initiation as a breakdown through runaway electrons and the 'traditional' approach assuming the development of positive streamer systems. For example, it is noted in [26] that the low-frequency electromagnetic response of compact discharges is a natural consequence of the runaway electron avalanche evolution. In turn, the authors of recent paper [27] interpret the original experimental results on CID observations and give a clear preference to the hydrometeor scenario of lighting initiation. The data in [27] indicate that the positive streamer breakdown in a thundercloud can be observed when the strong field is present in a relatively narrow altitude range, which is not sufficient for a runaway electron avalanche generation. The only fact on which advocates of both the mentioned approaches agree is that the questions of CID interpretation and lightning initiation are closely connected.

Importantly, the above approaches to the lightning initiation problem either fully ignore the existence of charged hydrometeors in the cloud environment or focus on the analysis of one or more particles. At the same time, as we see in what follows, the collective dynamics of charged hydrometeors that form the intracloud medium play a fundamental role in the lightning discharge initiation. The idea to consider collective effects in the plasma-like intracloud medium — the charged hydrometeor ensemble — was suggested by Trakhtengerts [28, 29], who introduced a simple two-component model for beam instability, which leads to intracloud medium stratification and the breakdown initiation. In subsequent studies [30–32], it was shown that under typical thundercloud conditions the collective modes of spatial discharge can form and be unstable for wavelengths from 10 to 100 m. The influence of the hydrometeor collective field on electron runaway effects in thundercloud was studied later in [33, 34]. We note that the effects of the intracloud medium quasi-electrostatic stratification play the key role during the initiation of compact intracloud discharges [35, 36].

In recent paper [37], the collective behavior of charged hydrometeors was investigated based on the noise it creates: a small-scale electric field, which fundamentally influences free electron generation. Free electron generation by the hydrometeor stochastic field in the absence of electrodes is regarded as a noise-induced kinetic transition. After 30 years of research, it became obvious that even a small noise can lead to qualitative changes in a system that is far from thermal equilibrium [38]. The noise sources may not decrease, but instead significantly increase the sensitivity of the system to weak external actions and induce regimes that cannot be realized without noise. A similar situation occurs in the thundercloud: the increasing charge and concentration of hydrometeors lead to a fluctuation decrease of the breakdown threshold in the cloud environment. This kinetic transition has a number of characteristic features, which are discussed in Section 3.1.

The collective dynamics of charged particles in a thundercloud reveal the conceptual depth of the simple definition of complex phenomena as systems whose behavior cannot be reduced to merely the sum of dynamic regimes of their components. The complexity of a thundercloud is primarily caused by the broad range of spatial–temporal scales of the ongoing electric phenomena. Characteristic spatial scales of the discharge-associated processes vary by at least 10 orders of magnitude from the interatomic distances important for electrification processes to several dozen kilometers, corresponding to the dimensions of a developed thundercloud. The time scales vary similarly, from several nanoseconds for single streamers to fractions of a second for developed lightning discharges.

On the other hand, the broad range of spatial–temporal scales of lightning discharges gives the key to understanding their main regularities. According to field measurement data, the dynamics of the electric structure of lightning discharge demonstrate unique scaling properties: they are self-similar in a quite broad range of spatial–temporal scales, which manifests itself in a strong correlation of the registered values, decreasing by a power law. This property is typical of critical phenomena; therefore, the electric discharge dynamics reveal properties of a self-organizing and self-tuning critical regime.

In other words, electric discharges in the atmosphere are related to systems with self-organized criticality [29, 32, 39]. These systems do not have characteristic temporal or spatial scales that would determine their evolution. Although the dynamic response of such systems is complicated, their statistical properties can be described by simple power laws in a specific parameter range. The discharge is a result of the thunder system balance on the threshold of some geometric phase transition, when the constant supply of free energy to the cloud is counterbalanced by the losses to fractal dissipative structures — fractal clusters, formed by the conducting channels generated during the discharge. Such a geometric transition is called the percolation phase transition; unlike conventional (thermodynamic) phase transitions, it is determined by the geometric properties of the conducting channels, a fact that suggest the use of modern methods of fractal geometry and percolation phase transition theory in the modeling of lightning discharges.

The attractiveness of the fractal approach to problems of lightning physics manifests itself in two aspects. First, the newest tools of fractal analysis are used for processing the field experiment data, including the results of satellite and multipoint ground observations. Second, the fractal approach as a mathematical language of the self-organizing criticality concept became the base for new approaches to modeling the dynamics thunder phenomena. Examples of the applications of the fractal approach to the description of electric discharge phenomena in thunderclouds are given in [40–42], where lightning discharge initiation models are constructed. The fractal approach was used to model both high-frequency and broadband fields of thunderstorm radiation [43, 44], which is formed by a complex of microdischarges generated during the formation and evolution of separate branches of the discharge structure.

The most important feature of the fractal approach to describing lightning discharge is its universality: in fact, this approach can be applied in the same way for any formation mechanism for the conducting channel if the macroscopic characteristics of the channel satisfy relatively simple and physically justified relations [45].

The uncertainty regarding the lightning initiation mechanism becomes more and more controversial as the capabilities of experimental investigations of the electric processes in the atmosphere constantly improve. Over the last few years, the rapid development of experimental devices has allowed various research groups to present results of lightning discharge observations with high spatio–temporal resolution. The data were obtained using innovative systems of high-frequency interferometry and radars with phased-array antennas. Many aspects of the obtained results cannot be properly interpreted in the framework of the existing approaches. A special role in electric discharge observations in the atmosphere is played by satellite registration systems, which are briefly reviewed in Section 2.

2. Satellites as unique instruments for detecting lightning discharge radiation

The beginning of the space era and the installation of sensitive detectors for various frequency bands on spacecraft opened new possibilities for observing lightning. The most intensive spectral components of the electromagnetic radiation generated by usual lightning discharges are the very-low-frequency ones (for intracloud and cloud–ground discharges). During propagation to satellite orbits, these components are strongly distorted and damped by the well-conducting ionosphere. Therefore, at the start, most attention was focused on the registration of the optical radiation of lightning discharges. The first devices of this type were the Optical Transient Detector (OTD) installed on the MicroLab-1 satellite (launched in 1995, later renamed OV-1) and the Lightning Imaging Sensor (LIS) installed on the Tropical Rainfall Measuring Mission (TRMM) satellite (launched in 1997). Both detectors registered radiation in the 777 nm wavelength, which allowed stable detection of lightning flashes, even through high spindrift clouds. The detectors were used for the long-time observation of global lightning activity, which provided answers to a number of very important questions of lightning climatology, including significant improvement in the understanding of the interconnection between troposphere convection and lightning activity at low latitudes, recording the most complete seasonal maps of the global distribution of lightning flashes, and obtaining reliable estimates of the density and rate of lightning discharges [1, 46, 47]. But because the mentioned spacecraft were in elliptical orbits, the observation time for a specific region on Earth's surface was from 90 s to several minutes, while the spatial location of the flash was determined with an accuracy from one to several kilometers and the time with an accuracy from 10 to 100 ms [48].

The next improvement in the optical observation of lightning flashes from space was associated with the launch of the currently most sophisticated geostationary meteorological satellite, GEOS-R (GEOS-16). Among various devices installed on this spacecraft is the Global Lightning Mapper (GLM) optical detector, which is based on experience in the development of the OTD and LIS detectors. The GLM detection quality was significantly improved: the spatial resolution increased to 8 km for nadir observations and to approximately 14 km for observations close to the region boundary, while the time resolution reached 2 ms [49]. The last fact allows the GLM detector to register spatial clusters of optical flashes corresponding to 2 ms time intervals. Moreover, unlike previous devices, the GLM has the capacity to continuously observe an arbitrary region on Earth's surface, which allows studying the correlations between troposphere convection and lightning activity over the whole lifetime of the thunder cluster.

As follows from the foregoing, the satellite systems for the registration of lightning optical radiation still do not have high enough spatio–temporal resolution and cannot reconstruct the parameters of single discharges. However, the radiation emitted by lightning contains not only the optical component caused by the strong heating of the discharge channels with high currents but also strong radio frequency components. As we have mentioned, the low-frequency band of this radiation is effectively reflected by the ionosphere, while the higher-frequency band (with frequencies above 15–20 MHz) experiences almost no scattering in the ionosphere, and its influence can be mainly reduced to dispersive distortions of the signal. It was the VHF range between 30 and 300 MHz where several spacecraft registered quite unusual short high-power signals. The mechanism of the generation of these signals remained unknown for many years; however, there was no doubt about their tropospheric origin or their connection with the electric discharges in thunderclouds. We analyze these signals in more detail and show how their properties can be connected with the parameters of the corresponding discharges.

The first signals with paired bursts of strong high-frequency radiation were registered by the Blackbeard broadband radio-frequency detector installed aboard the ALEXIS (Array of Low Energy X-ray Imaging Sensors) microsatellite launched in 1993 [50–52]. In the broadband detection regime, the Blackbeard detector recorded radiation in the 65 MHz frequency band in the frequency intervals 25–95 MHz and 108–166 MHz. The analysis of more than 500 events of this type allowed concluding that their source is located below the ionosphere, which was evident from the dispersion of the paired pulses in dynamic spectra. Therefore, in [50, 51], these bursts were named Transionospheric Pulse Pairs (TIPPs).

According to [50, 51], the TIPPs in the 28–90 MHz frequency range are radiation bursts with a duration from 1 to 20 μs (average duration 2–4 μs) separated by a time interval from 10 to 100 μs (the average interval being 50 μs). The pulse intensity exceeded the background level by 20–40 dB and the pulse power in the considered band was at least one order of magnitude higher than the radiation power of a typical lightning discharge. The statistical characteristics of TIPPs in the 117–166 MHz range were almost no different from those in the lower part of the VHF band (from 30 to 300 MHz), except for lower dispersion and the time delay between the pulses reaching 37 μs [52]. In both low-frequency and high-frequency ranges of the VHF band, there were usually the observations of lightning discharge radiation during the registration of pulse pairs (for exposures from 7 to 100 ms).

The authors of [50–52] suggested two mechanisms of the generation of the second pulse. The first was that the second pulse is a reflection of the radiation emitted by a pulsed high-altitude source from Earth's surface. The second was that the pulses were emitted by different correlated sources with an unknown coupling nature. A further comparison of the ALEXIS satellite data with multipoint ground registrations of lightning discharges has shown that the high-frequency pulse sources are connected with thunderclouds, and the second pulse is most probably emitted by some source and is then reflected from Earth's surface.

The capability to detect radiation from compact intracloud discharges was significantly enhanced with the launch of the Fast On-orbit Recording of Transient Events (FORTE) satellite in 1997 [53]. The satellite detectors allowed registering radiation at frequencies from 26 to 49 MHz simultaneously for two different polarizations or for one polarization but simultaneously in the 26–49 and 118–151 MHz ranges. Moreover, FORTE was also equipped with sensitive optical sensors. Satellite registration of TIPPs with an unknown source location provided a ratio between the source heights for different events, which together with the geographical coordinates of the discharges gave a height value [54] under the assumption that the second pulse is the reflection of the initial (first) pulse from Earth's surface. Geographical coordinates of the discharge were determined by electric field observations in VLF/LF bands (at frequencies from 3 to 300 kHz) at the multipoint systems LASA (Los Alamos Sferic Array) and NLDN (National Lightning Detection Network).

The analysis of ground and satellite measurement data on compact discharge radiation allowed determining their location, height, and optical brightness. Most importantly, by simultaneously registering events in the VLF/LF and HF/VHF bands with an accuracy of the FORTE position determination, it was shown that the sources of the short bipolar electric field pulse and the transionospheric pulse pair coincide in space and time [55, 56]. It was also shown that TIPPs with an effective power greater than 40 kW in the 26–48 MHz frequency range and the duration of 3–5 μs are weakly polarized and incoherent. These pulses are either observed isolated from other electrical phenomena in the cloud or precede a usual intracloud discharge, which emits much weaker radiation in the VHF band than the CID does [55, 57].

Under simultaneous registration of CID radiation in the low-frequency (using the LASA system) and high-frequency (the FORTE satellite) bands, it was discovered that the number of TIPPs exceeds the number of short electric field bipolar pulses. Usually, the VHF radiation pulse of a compact discharge is not accompanied by the low-frequency component when the CID initiates the intracloud discharge and the leader formation. On the contrary, if the high-frequency pulse is accompanied by a short bipolar electric field pulse, then the intracloud discharge is not generated [57]. Independently of electric field bipolar pulse generation, the CIDs emit in the optical range very weakly with respect to ordinary lightning discharges [58], and hence the observed high-power short burst of high-frequency radiation has almost no synchronous optical component.

Important data on the high-frequency CID radiation were obtained during the quite successful mission of the Russian Chibis-M microsatellite, which started its operation in orbit in January 2012 [59]. It was initially intended to use Chibis-M for the investigation of lightning discharges, and its scientific measurement system therefore included a radiofrequency analyser (RFA) with the frequency band 26–48 MHz, X-ray, gamma, and UV detectors, and a digital camera. Over two and a half years of operation, Chibis-M registered more than 400 high-power bursts of high-frequency radiation.

One of the most important results obtained during the Chibis-M mission is that there are numerous thundercloud events that lead to the generation of morphologically different high-frequency spectra. Unlike the spectrograms obtained with the ALEXIS and FORTE satellites, the Chibis-M spectrograms of high-frequency signals have a more complicated structure. First of all, besides pairs of

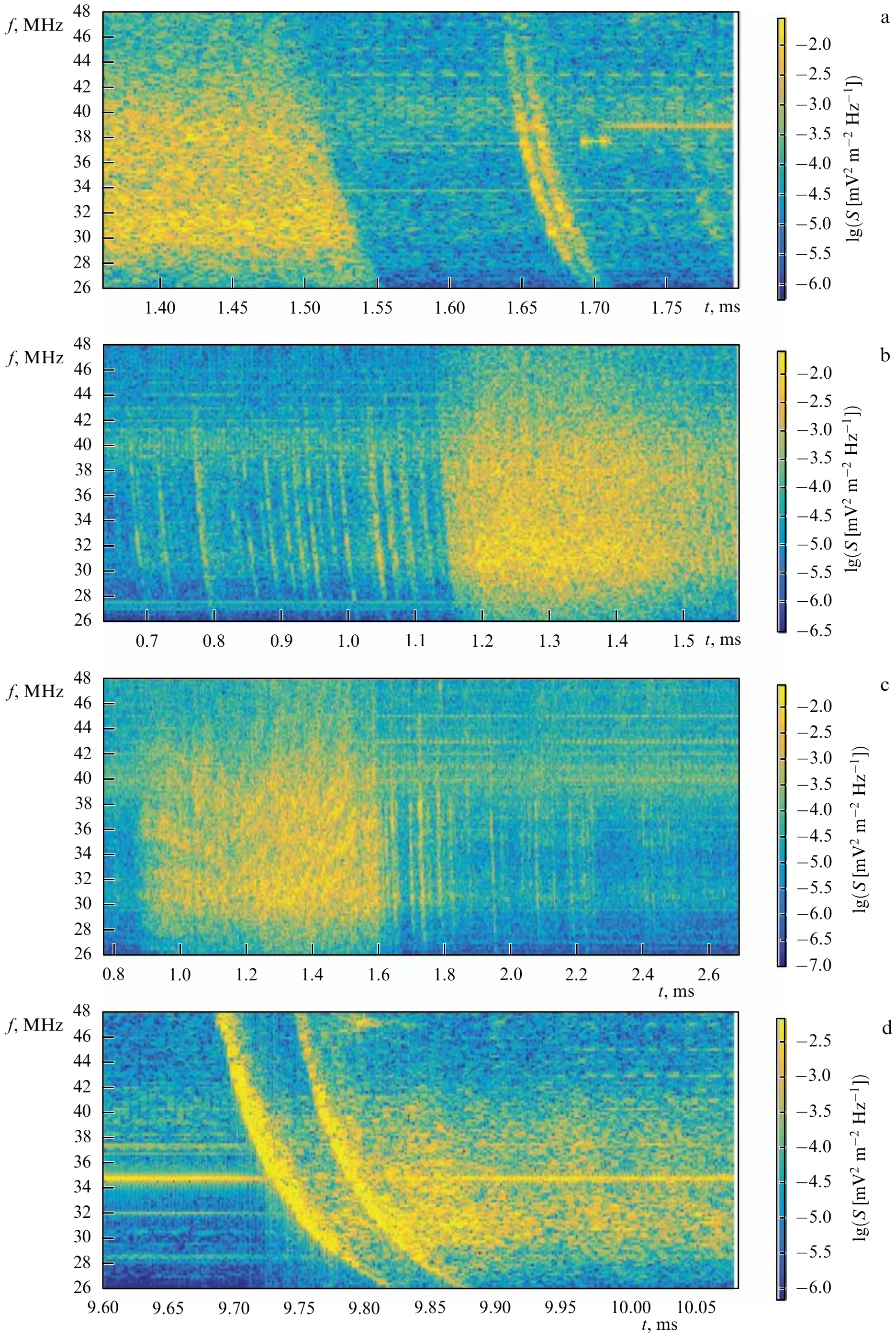

Figure 1. Spectrogram examples of high-frequency signals of an atmospheric origin registered aboard the Chibis-M microsatellite: (a) January 8, 2012 at 17:31:56 UT (Universal Time), (b) January 9, 2012 at 22:42:10 UT, (c) April 9, 2012 at 21:29:38 UT, (d) November 4, 2013 at 15:05:03 UT.

short and strong radiation bursts, large areas of the spectrograms contain long (sometimes over several dozen milliseconds) and intense noise radiation, which can start and end with a high-power short burst (or with a series of short bursts) or can start and end unrelated to the burst instant. In addition, during some of the events, the noise radiation was not accompanied by short bursts at all, and single bursts were sometimes observed instead of pairs (Fig. 1) [60]. Obviously, it is impossible to interpret the mentioned spectra assuming that of the radiation source is a single linear current burst. But these results can be interpreted if the discharge is viewed as a fractal dynamic structure of conducting channels that develops in an inhomogeneous electric field of a thundercloud (see Section 3.2).

In describing satellite observations of high-frequency atmosphere radiation, we must note one of the most mysterious phenomena, so-called terrestrial gamma-ray flashes (TGFs). They were discovered during the Burst and Transient Source Experiment (BATSE) aboard the Compton Gamma-Ray Observatory (CGRO) launched in 1991 [61], and they have a shorter duration (up to several milliseconds) and a more rigid energy spectrum than cosmic gamma bursts. The largest number of gamma bursts of terrestrial origin was registered during the Reuven Ramaty High Energy Solar

Spectroscopic Imager (RHESSI) [62] and Gamma-ray Burst Monitor (GBM)/Fermi [63] orbital missions. Moreover, TGFs were registered in space experiments at AGILE (Astro-Rivelatore Gamma a Immagini Leggero) [64, 65], and LAT (Large Area Telescope)/Fermi [66], as well as by the SONG-D detector during the AVS-F experiment aboard the CORONAS-F spacecraft [67] and DRGE detectors on the Vernov satellite [68]. It was initially assumed that the TGF sources are sprites, which were discovered shortly before the first TGF registration [69], but now the possible sources of these gamma bursts of terrestrial origin are considered to be lightning discharges between clouds and intracloud discharges, including CIDs. Many properties of TGFs, which are important for the development of a self-consistent theory of this phenomenon, are still unclear, including the source directivity diagram, its dimensions, and the altitude and the rate of TGF occurrence and its connection with various types of lightning.

3. New approaches in the lightning discharge theory

3.1 Lightning initiation as a noise-induced kinetic transition

As we mentioned in the Introduction, noise-induced kinetic transitions play an important role in the statistical physics of nonequilibrium processes: noise sources may not just decrease, but instead significantly increase the system sensitivity to weak external actions and induce some regimes that are unrealizable in the absence of noise [38, 70–72]. A similar situation occurs in a thundercloud: an increased concentration of hydrometeor charge leads to an increase in the intensity of quasi-electrostatic noise and to a fluctuation decrease in the cloud environment breakdown threshold [37]. This means that even exponentially rare bursts of the supercritical field (ionization center) $\nu_{\mathrm{i}}(\mathbf{r}, t) = \nu_{\mathrm{i}}(E(\mathbf{r}, t) \gtrsim E_{\mathrm{b}}) \gtrsim \nu_{\mathrm{a}}$ can provide an exponential increase in the number of free carriers if the ionization rate averaged over time and space is much less than the attachment rate: $\langle \nu_{\mathrm{i}}(\mathbf{r}, t)\rangle / \nu_{\mathrm{a}} \ll 1$.

It is essential to note that a major role in the realization of the subthreshold generation of free carriers is played by correlation effects. For example, if two ionization centers occasionally appear close to one another in space and time, then, besides the independent increase in the electron concentration (free carriers), the two centers demonstrate an additional increment. This increase occurs because the exponential growth in the electron (free carrier) number at the second center starts not from the space-averaged concentration at that instant but from a higher level, the electron (free carrier) concentration spot left after the first center.

The pulsed character of the ionization center behavior in the intracloud environment dynamics leads to quite a significant reduction in the exponential increase threshold compared with that in the case of a constant electron multiplying rate. However, even such a strong decrease in the explosive instability threshold may not be enough in the case of high electron losses due to attachment. The reason lies in the fact that both the attachment rate and especially the ionization rate strongly depend on the external electric field: a decrease in the field amplitude by λ times with respect to the breakdown value E_{b} leads to a reduction in the ratio between the ionization and the attachment rates by approximately λ^5 times [73]. In other words, even a fourfold field decrease leads to a reduction in the average ionization rate by several thousand times.

The solution is given by the knowledge of stationary glow discharges in electronegative gases [8]. It turns out that quasi-stationary discharge development at large timescales that exceed the spark discharge development time lead to the accumulation of active particles that destroy negative ions and release the trapped electrons. Detachment processes partially compensate the attachment effects and thus decrease the electron losses. In other words, electrons appearing in the multiplying centers are very rapidly included in some depository of negative ions, which at time scales of the inverse detachment rate ν_{d}^{-1} becomes a free electron emitter itself.

We note that the elementary charge kinetics in the negative-ion depository appear to be quite complicated: each ionization burst with rapid electron attachment to oxygen is followed by relatively fast recharge reactions leading to the O_2^- ion transformation into ions with a higher electron binding energy: O_3^-, NO_3^-, or aquated ions $NO_3^-(H_2O)_n$ in moist air [74]. This means that the breakdown field reduction in a thundercloud is connected with the fluctuation decrease in the threshold for the exponential growth in the negative-ion concentration n_{n}, which in turn increases the electron concentration n_{e} due to the detachment:

$$\frac{n_{\mathrm{e}}}{n_{\mathrm{n}}} = \frac{\nu_{\mathrm{d}}}{\nu_{\mathrm{a}}} \,. \tag{1}$$

It is essential that the electron multiplying at ionization centers close to the threshold now acts not against the attachment but against the recombination losses, which are slow and insignificant for positive-ion concentrations $n_{\mathrm{p}} \ll 10^{19}\ \mathrm{m}^{-3}$.

Another important manifestation of the fluctuations of the charged hydrometeor small-scale electric field is the randomization of the electron and ion drift velocities. Precisely the advective removal of ions plays the key role in the realization of the considered lightning discharge initiation mechanism: the threshold for the exponential increase in the ion concentration is determined by the appearance of the connected geometric component in the ensemble of negative-ion density bursts that overlap in the spatio–temporal continuum. The dimensionless burst concentration is defined by the expression

$$\mathfrak{B} = \frac{\pi^2}{2}\, L_{\mathrm{n}}^3 \tau_{\mathrm{n}} \mathfrak{M} \,, \tag{2}$$

where $\mathfrak{M}$ stands for the appearance rate of over-critical random field bursts per unit volume and time exceeding the breakdown field $E(\mathbf{r}, t) \geqslant E_{\mathrm{b}}$. The connected geometric component in the overlapping ion concentration burst ensemble appears due to the percolation phase transition, when the dimensionless concentration of bursts $\mathfrak{B}$ reaches the critical value of approximately 13% (Fig. 2).

3.2 Lightning discharge as a fractal dissipative structure

The view of discharge as a fractal probabilistic evolving system of conducting channels allowed describing a number of important electrical properties and morphological features of lightning discharges (see, e.g., [41, 42] and the references therein). In the framework of this approach, the conducting structure that forms during the discharge plays the role of a

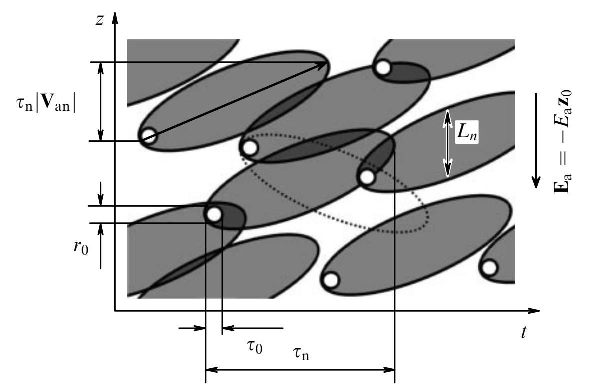

Figure 2. Schematic image of the spatio–temporal dynamics of overlapping ion density spots. White circles correspond to the ionization centers; grey ellipses correspond to the negative-ion density spots and are stretched along the direction $z = |\mathbf{V}_{an}|\, t$. The dashed ellipse corresponds to the positive-ion density spot and is stretched along the direction $z = -|\mathbf{V}_{ap}|\, t$ [37].

drainage system for fast electric charge collection from huge volumes of thunderclouds. This allowed describing the charge transfer, channel conductivity dynamics, and hence the discharge current structure. As a result, qualitative models of discharge were built. These models provided good agreement with the observations and described the morphology, currents, velocity, and propagation character of different types of charges. Notably, such a discharge model was used to describe the influence of the lower positive layer on the development of intracloud and cloud–ground discharges [42], as well as to analyze the structure and dynamics of compact intracloud discharges [35, 36]. A short description of the main aspects of this model is given below.

The "intracloud electrified medium–lightning discharge" system is regarded as a three-dimensional region with spatial charges connected by an evolving system of conducting channels. Each point of an equidistant spatial grid contains a value equal to the electric charge accumulated in the corresponding elementary cell. The amount of charge in the cells at the initial instant is determined by the intracloud electric field distribution. The distribution of elementary charges at the initial and all subsequent instants determines the electric potential at each point of the grid and hence the electric field between adjacent points. The charge dynamics in each cell are defined by the existence of electric connections with the adjacent cells (conducting channels) and by their characteristics. It is assumed that the possibility of a conducting channel appearing (breaking down) between adjacent i and j cells increases with the electric field strength E_{ij} between them and is described by the Weibull distribution [75]:

$$P(E_{ij}) = \begin{cases} 1 - \exp\left(-\left|\dfrac{E_{ij} - E_{\mathrm{i}}}{E_{\mathrm{c}} - E_{\mathrm{i}}}\right|^m\right) & E_{ij} \geqslant E_{\mathrm{i}}\,, \\ 0, & E_{ij} < E_{\mathrm{i}}\,. \end{cases} \qquad (3)$$

Here, m is the Weibull index, and E_{c} and E_{i} are the critical field and the charge initiation field, depending on the discharge type ($E_{\mathrm{c}} > E_{\mathrm{i}}$). If there is a conducting connection between adjacent cells, the electric current between them is determined at each step of the modeling time by the connection conductance and the electric field strength, while the variations in the electric charge in each cell are determined by the sum of incoming and outgoing currents. An important feature of the model is that the dependence of the channel conductance on the current flowing through it is taken into account: the main factors determining the channel conductivity are its ohmic heating and the effective cooling, which are described in the framework of a differential analogue of the Rompe–Weizel formula [76]. We note that if the conductance of the channel decreases to a value close to the initial one, then the channel disappears.

This model describes the emergence and the evolution of a hierarchical structure of conducting channels in the intracloud medium in the presence of an external electric field and the initial inhomogeneous charge density distribution. The emerging current system is a distributed stochastic source of electromagnetic radiation, with its elements being the linear currents between adjacent cells.

Importantly, this model takes the microphysics and the properties of the discharges into account only in the form of general relations and relatively simple parameterizations. Nevertheless, it provides interpretations for the morphology, electric properties, and electromagnetic radiation of lightning discharges of various types for the corresponding choice of the channel characteristics, cell dimensions, and the model time increment. It is quite reasonable to assume that the discharge representation in the form of a cellular automaton network is currently the only way to describe its macroscopic evolution, because the traditional three-dimensional calculations of the discharge behavior are still far from perfect and require large computing resources, even for the calculation of the dynamics for single elements of the discharge [77]. Nor do they describe the macroscopic current system of the considered phenomenon or reveal a number of key characteristics, particularly the degradation and the branching of discharge channels. Moreover, the introduction of fractal geometry methods to describing the processes in strongly nonequilibrium systems and the detailed consideration of cluster–cluster aggregation effects are very promising for the construction of a general theory for the broad variety of electric processes, from lightning initiation to transient luminous events (TLEs).

3.3 Compact intracloud discharge model as an example of applying a new approach for describing discharge phenomena

The fractal discharge model described in Section 3.2 resulted in a significant progress in the understanding of the evolution of and electromagnetic radiation emission from such an unusual process as CIDs. Among all various lightning activity effects, the CIDs are special. The term 'compact' was attributed to these discharges due to their small spatial length, which is estimated to be several hundred meters. CID radiation in the far field consists of a narrow bipolar pulse (NBP) of the electric field with a characteristic duration of 10 to 30 μs and a synchronous high-frequency radiation burst with an even shorter duration and with a power reaching several dozen gigawatts, which is one order of magnitude higher than during a typical cloud–ground discharge. This fact makes these discharges the brightest natural sources of radio waves in the HF/VHF band.

Despite intensive experimental and theoretical investigations, which have been ongoing since the discovery of this type of discharge in the 1980s [78], CID is still one of the most mysterious phenomena in lightning activity. Various features of the CID structure and radiation have been interpreted within different models based on the runaway electron

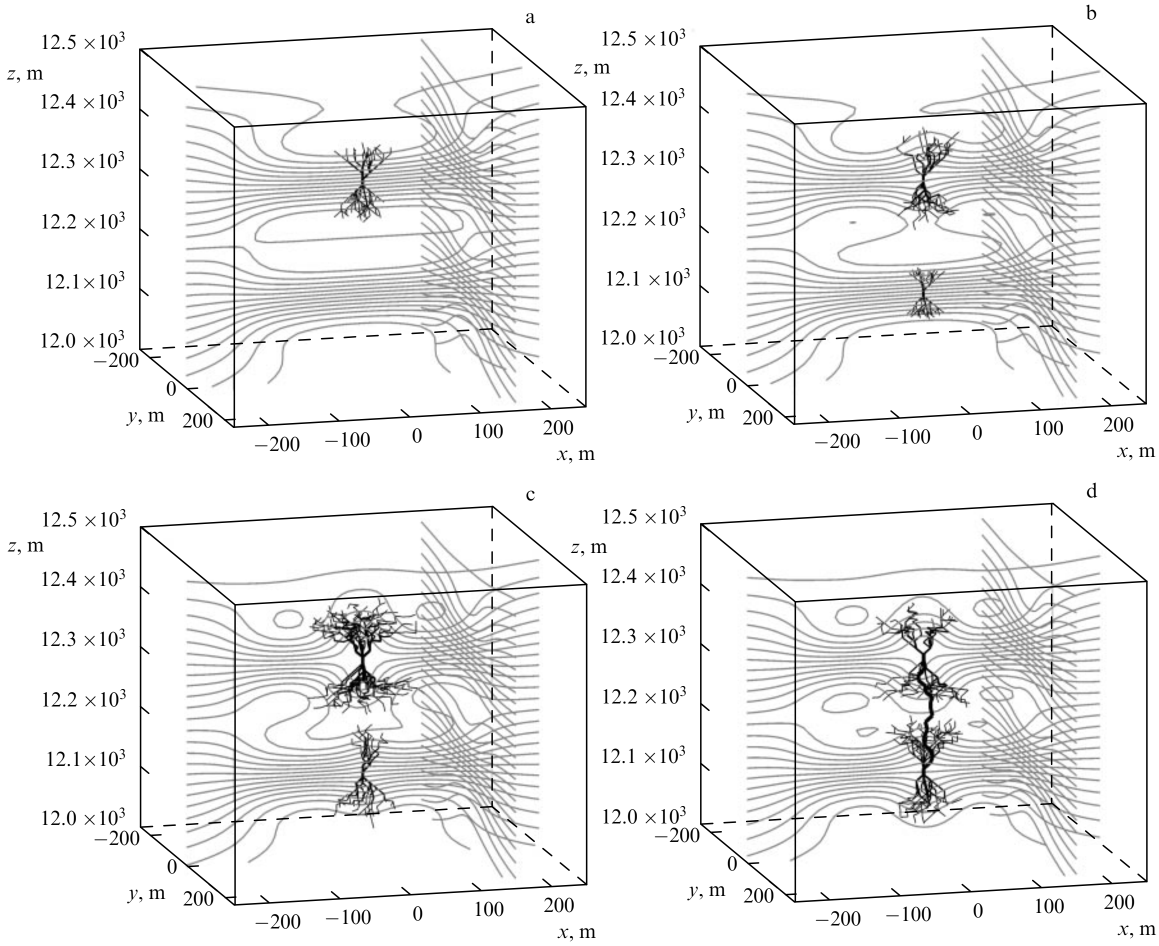

Figure 3. Successive stages of the CID evolution in a medium with a spatially inhomogeneous external electric field: (a) development of the first streamer discharge after seven model time steps (time $t = 140$ μs); (b) initiation of the second discharge ($t = 3.06$ s); (c) simultaneous development of the discharge pair ($t = 7.50$ s); (d) instant of electrical contact between the discharges after 556 steps of the model time ($t = 11.12$ s) with high-current channel formation. Grey curves correspond to equipotentials in the planes $y = 0$ and $x = 150$ m [36].

breakdown evolution [18, 79], instantaneous elongation of the leader channel [80], or instantaneous generation of a single propagating current pulse [81].

Relatively recently, a new mechanism of CID generation was suggested in [35, 36]. This mechanism is based on the fractal approach to describing CID: compact discharge is regarded as a result of the interaction between two or more bipolar streamer structures that evolve in a large-scale inhomogeneous external electric field of a thundercloud. This approach provided a self-consistent interpretation of the features of low-frequency and high-frequency CID radiation, as well as the spatial structure of CIDs. We consider this in more detail.

The approach described in Section 3.2 has a number of features in application to compact discharges. The problem is that a short and powerful burst of CID radiation does not correspond to the parameters of a typical intracloud discharge, which has a much longer duration and emits much less radiation, in both the low-frequency and high-frequency ranges. All known mechanisms fail when trying to explain the magnitude of the source current needed to generate such radiation (similar to the return stroke during a cloud–ground discharge) and its vertical span (not more than several hundred meters) [82]. These features can be explained under the assumption that the CID has two stages: a preliminary one and the main one. During the preliminary stage, two bipolar discharge structures evolve at a relatively small vertical distance from each other, with their vertical size and location being determined by the inhomogeneity scale of the initial electric field (Fig. 3).

Because the relative increase in the electric field in the CID generation region over the initiation field is small, it is assumed that the conducting structures are formed by streamer-type discharges during the preliminary stage (see recent paper [83]). The development time of these structures is much greater than the CID radiation burst duration, and in the course of evolution they accumulate significant electric charges with different polarities on their opposite ends (at the discharge coronas). The electromagnetic radiation of the initial stage is weak due to relatively low currents and low conductivity of the discharge structure.

The second and main stage of compact discharge starts when the oppositely charged coronas of the discharge structures come into electric contact. The breakdown during the main stage occurs in a preliminarily ionized medium with a strongly inhomogeneous distribution of the electric current density, which allows assuming that the ionization wave mechanism is responsible for the formation of a conducting channel, analogous to a similar process during the return stroke in a cloud–ground discharge. The most important feature of the ionization wave is an abrupt decrease (by several orders of magnitude) in the discharge channel resistivity after the wave front passes, which results in the heating, ionization, and gas-dynamic expansion of air. The ionization wave propagates upward and downward from the contact point with a current burst in the channel being caused by the fast charge collection from the elementary cells through which the channel passes during a short time interval. The net charge of the channel tends to zero.

An important feature of the CID main stage is the active branching of the discharge channel in regions with a high charge density formed during the preliminary stage of the CID. Assuming that the ionization wave velocity during the CID main stage equals the typical velocity of the current burst during the return stroke, we can obtain good agreement between the calculated electric field bipolar pulse and the observation results [81, 82]. The current pulse generated during the main stage corresponds in duration and amplitude to the return stroke current during the cloud–ground discharge, while the high-power short burst of the high-frequency radiation is associated with the formation of new highly conducting channels (breakdown) between the adjacent cells of the discharge structures. This means that the main features of CID radiation have an explanation as a cluster–cluster aggregation of discharge structures in the thundercloud.

The scenario considered above for the compact discharge evolution assumes, first of all, the existence of an initial middle-scale inhomogeneity of the charge density and hence of the electric field. Such an inhomogeneity formation can be caused either by the turbulent component of the convective flow, which is enhanced close to the upper boundary of the cloud, or by the flow instability first described in [28]. This instability forms inside a multicomponent intracloud environment with the existence of a weakly conducting airflow with respect to heavier intracloud particles. As a result, an exponentially growing spatial charge wave forms inside the cloud and moves together with the convective flow toward the cloud top. The growth increment and the spatial scale of the appearing charge density inhomogeneity depend on the charge, mass, and concentration of heavy particles, on their effective collision rate, and on the specific conductivity and relative velocity of the airflow. According to the estimates in [28], the characteristic time for instability to set in is of the order of 100 s, and the spatial scale of the inhomogeneity can vary from several dozen to several hundred meters.

It is important that the considered mechanism for the electric field inhomogeneity formation is quite stable with respect to the heavy particle characteristics and to the magnitude of the external electric field. Recently, it was shown experimentally that such particles could be present even in the upper layers of the developed thundercloud [84]. The significant influence of local convective fluxes on CID formation is supported by the observed spatio–temporal clusterization of compact discharges. This process reveals itself in an abrupt sharp increase in the CID appearance rate in a bounded region close to the lower boundary of the thundercloud screening layer [85].

We note that the existence of medium-scale spatial modulation of an initial electric field distribution allows naturally solving the problem of spatio-temporal synchronization of the discharge structures at the initial stage of the CID, which is important for their subsequent electrical contact. Because the electric field near the discharge structure edges increases during the discharge evolution, the adjacent field maximum also grows, which in turn increases the probability that a second structure would form in the vicinity of the adjacent field maximum at a distance up to several hundred meters from the first structure. In this case, before the instant of contact, both structures that were initially separated by the weak field region have time to accumulate an electric charge that suffices for the formation of an observable main stage of the CID.

The calculation results for the structure and electromagnetic radiation of a typical small CID, which appears close to the upper boundary of the main positive layer (at a height of about 12 km), are given in [35, 36]. In the considered example, the second discharge occurs at the preliminary stage with a delay of approximately 5 ms after the first discharge initiation (Fig. 3a, b). After that, both discharges coexist for a long time (Fig. 3b, c). As a result of the discharge redistribution (the current in each discharge does not exceed 22 A and the full transferred charge is approximately 0.1 C), the electric field drop between the discharge structures decreases until the instant (approximately 11 ms after the second discharge initiation) when the streamer structures come into electric contact and the main stage of the CID starts (Fig. 3d). The discharge that evolves during the main stage neutralizes the electric charges that accumulated during the preliminary stage on the opposite edges of the discharge structures. This leads to the generation of a current pulse with a 40 kA amplitude and several microsecond duration. The pulse is accompanied by an intensive branching of the channel close to the regions with high charge density.

When calculating the CID electric field, it is natural to assume that the low-frequency component of the current system radiation is determined by its slowly changing large-scale component, while the high-frequency radiation is connected with the electric breakdown between adjacent cells, i.e., with the formation of new conducting channels. The radiation emitted by each elementary linear current is determined by the length and the orientation of the discharge gap, the propagation speed, and the shape of the current pulse [86]. The calculations in [36] indicate that in ground observations, the only significant electric field component during the preliminary stage is the electrostatic component, reaching 0.45 V m^{-1} close to the discharge at a distance not more than 10 km from its axis. All other field components are small during the preliminary stage and cannot be reliably measured in present-day experiments.

During the main stage of the CID, there are different dominating components of the electric field at different distances from the discharge axis, unlike the single dominating component during the preliminary stage. Almost right below the discharge, the induction component is dominant, exceeding 3 V m^{-1}, but already at a distance of 10 km from the discharge axis, the radio component becomes the maximal one and reaches almost 35 V m^{-1}, while the induction component decreases to 0.8 V m^{-1}, and the static component does not exceed 30 V m^{-1}. The same relation between the components persists at larger distances from the discharge. At a distance of 100 km from the discharge, the radio field component has the form of a single pulse and has an amplitude of approximately 14 V m^{-1} (Fig. 4a).

The temporal realization of the high-frequency component of the ground electric field at a 100 km distance from the discharge and its spectrum are shown in Fig. 4. The level of high-frequency radiation at the main stage of the CID turns

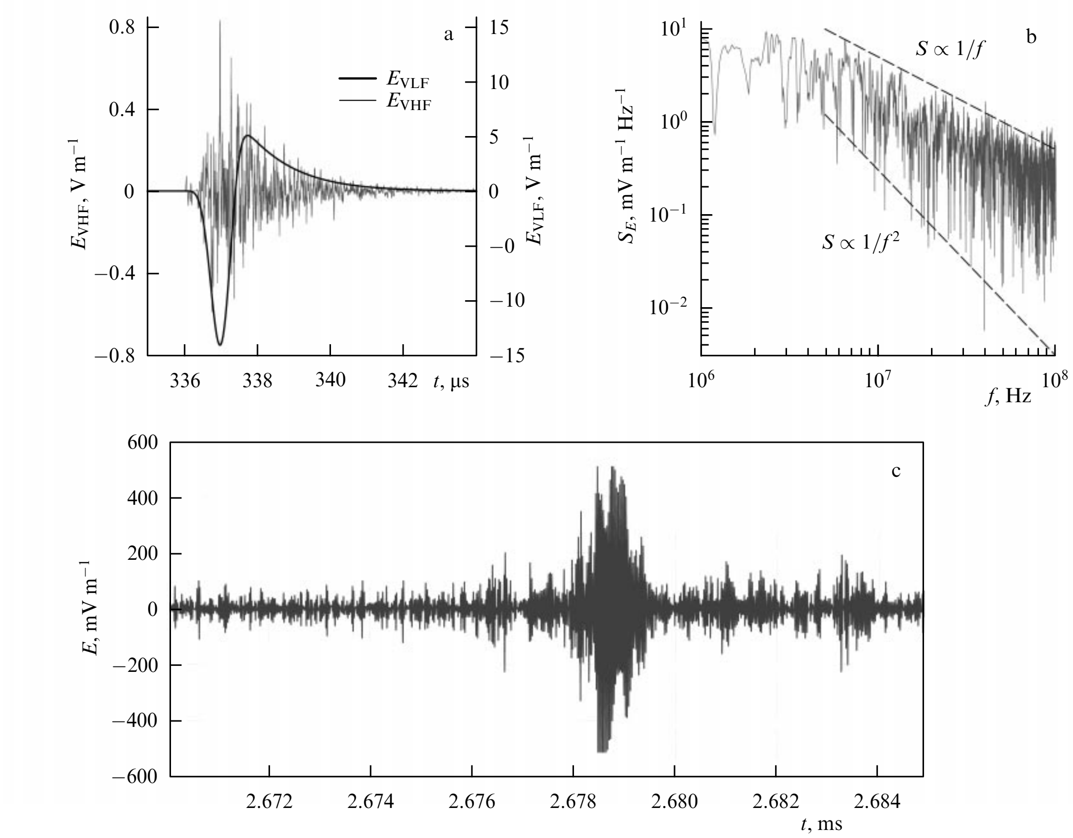

Figure 4. (a) Temporal realization of the high-frequency electric field component E_{VHF} shown together with the synchronous short pulse of the low-frequency electric field E_{VLF} (smooth curve) during the main stage of a CID and (b) the high-frequency field component spectrum at a distance of 100 km from the discharge axis [36]. (c) An example of a short high-power burst of high-frequency radiation recorded aboard the Chibis-M satellite on 19.08.2012 at 04.31.31 UT.

out to be several orders of magnitude higher than at the preliminary stage. Moreover, Fig. 4a illustrates the synchronous timing of the high-frequency radiation burst and the low-frequency electric field bipolar pulse. The high-frequency radiation spectrum, as clearly seen in Fig. 4b, lies between two frequency dependences of the forms f^{-1} and f^{-2}. The upper boundary corresponds to the spectrum of a critical dynamics process, while the lower one is connected with the existence of several independent realizations of such processes in a discharge with normally distributed intensity.

CID radiation calculations in the framework of the fractal model considered above show good agreement with the observation results. First of all, the electromagnetic field at the preliminary stage of the CID turns out to be small in the model: in most cases, there are no indications of electric activity in the thundercloud before and after the compact discharge. The values of the duration and amplitude of the electric field pulse in the far field obtained in numerical experiments (up to several dozen microseconds and up to several dozen volts per m at a distance of 100 km from the discharge), as well as the instant of charge variation (up to several dozen Coulombs) correspond to measurements for typical compact discharges.

We note that the given parameters of the compact discharge radiation significantly depend on its length, i.e., practically on the vertical profile of the electric field perturbation in the CID region. Concerning a short high-power burst of high-frequency radiation, we can say that its intensity and duration are in good agreement with ground observations, while the power spectral density corresponds to characteristics of the atmospheric high-frequency signals recorded by satellites and known as transionospheric pulse pairs, which are direct and Earth-reflected CID signals [50].

To summarize, the suggested fractal model allows interpreting important features of CIDs, including weak radiation during the preliminary stage, the formation of a short bipolar pulse of the electric field, and the synchronous high-power burst of high-frequency radiation. Due to the specifics of the spatiotemporal structure of the discharge current, which expands upward and downward from the point of electric contact of discharge structures, the far-field electric field pulse remains narrow in a broad range of discharge parameters [36]. We note that the known CID models (see [18, 78–81]) do not provide a self-consistent description of this phenomenon.

4. Conclusions

A theoretical description of the initiation and evolution of electric discharges in thunderclouds is currently encountering fundamental difficulties, which were briefly discussed in the Introduction.

The historically established approach based on 'growing' a full discharge from a single microbreakdown in a strong external electric field makes it impossible to overcome these problems, as directly noted by the authors of recent papers on streamer discharge modeling (see, e.g., [9]). Moreover, as the technical capabilities for ground and satellite observations of lightning discharge radiation evolve, new experimental events are recorded, and these cannot be interpreted in the framework of the existing models of lightning discharge evolution. Striking examples of such observations are the short high-power bursts of high-frequency radiation, first recorded in the 1980s, that appear simultaneously with the short bipolar pulses of the low-frequency electric field. The generation mechanism of these pulses is still a subject of intense discussions (see the review of the corresponding investigations in [35]).

Difficulties in the theoretical description of lightning discharges and the interpretation of their broadband electric radiation obviously indicate the need to develop new approaches to solving these problems. The main aspects of one such approach were given in Section 3, and they include, on the one hand, a mechanism of conducting channel formation inside a cloud based on the electrostatic noise-initiated kinetic transition [37] and, on the other hand, a universal mechanism of their evolution based on cluster–cluster aggregation of the dynamic fractal conducting structures. This approach allows solving a number of very important problems in theoretical modeling of lightning discharge, which include justification of the lightning initiation mechanism in subthreshold average electric fields of a thundercloud, a natural interpretation of the morphology and evolution of the discharge [42], and a self-consistent description of its electromagnetic radiation.

Evidence for the effectiveness of this approach is the ability to use it for constructing a fractal model of a CID [35, 36]. This model describes the CID as a result of an interaction between two (or more) developed conducting discharge structures that were formed during the preliminary stage in a strongly inhomogeneous electric field of a thundercloud (see Section 3.3). The calculation results for the electromagnetic radiation emitted by the current system of such a discharge demonstrate good qualitative and quantitative agreement with the observations (see Figs 1 and 4). In particular, the emission of a model source turns out to be negligible during the preliminary stage of the discharge, while, during the main stage, which starts as the developed conducting structures come into contact, the emission consists of a high-power short burst of high-frequency radiation and a synchronous bipolar pulse of the low-frequency electric field. We note that this is the first example of a self-consistent description of the low-frequency and high-frequency CID radiation components that is in good agreement with observations.

An important feature of the suggested approach is the possibility of realizing different scenarios for the lightning discharge evolution, which leads to a significant difference in the electromagnetic signature. For example, the structure of a compact discharge at the preliminary and main stages, as was noted in [36], can generally be different from the tree-like one and represent a group of relatively low-current small-scale discharges, which appear in the whole region with a strong electric field. In this case, not every discharge reaches the full leader stage due to the low channel current. This, on the one hand, leads to the absence of detectable optical radiation (see [58]) and, on the other hand, provides a short high-power burst of high-frequency radiation with wavelengths of the order of the emitting conducting channel (from 1 to 10 m [8], which corresponds to the frequency range 30–300 MHz).

We note that this scenario for the compact (distributed) discharge evolution is in good agreement with the high-frequency interferometry data in [27]. Moreover, in the framework of the considered approach, it is possible to naturally interpret continuous intensive high-frequency noise, which either accompanies short high-power radiation bursts or appears alone. Indeed, during the preliminary stage development, small-scale charges in a single long region with a high enough electric field can generate long-term noncorrelated high-frequency noise radiation, while the CID main stage cannot even be reached, which is mostly determined by the initial electric field distribution. Precisely this type of structure is present in most of the high-frequency dynamic spectra registered aboard the Chibis-M satellite (see Fig. 1).

Obviously, many assumptions and conclusions related to the application of the above-described new approach to the modeling of electric discharges in thunderclouds require further theoretical and experimental investigations. Therefore, the most important role is played by satellite observations, which are a unique source of information about the spatio–temporal structure and the directivity diagram of the high-frequency radiation from lightning discharges of different types. This information a priori plays a role in solving the inverse electrodynamic problem — building a discharge model based on its electromagnetic emission — and allows estimating the characteristic dimensions and lifetimes of the discharge conducting channels, the electric charge dynamics, and the dependence of the discharge channel conductance on the value of the current flowing through them.

A significant amount of data on lightning discharge observations was obtained with the already ended missions, such as FORTE and Chibis-M. Despite the necessity to further process and systematize the obtained data, it is already obvious that in order to interpret it, new physical models of the discharge must be implemented. Besides the problem of high-frequency noise generation described above, a separate interpretation is needed, especially for the inconsistency between direct and reflected CID signals: according to [87], the reflected signal is often more powerful than the direct one and usually has a different temporal structure, in which the discrete components are clearly visible. It seems that in order to resolve this inconsistency, one needs a more detailed description of the CID radiation directivity diagram, with its morphology taken into the account.

Important open questions also include the dependence of the short high-frequency radiation burst characteristics on the geographic coordinates of their source and on the characteristics of the local troposphere convection. A separate important question is the correlation degree between short high-power high-frequency bursts or lightning activity in general and gamma-flashes of terrestrial origin [88]. Despite the assumption made in a number of papers about the connection between TGFs and special types or stages of lightning discharges, there is still no reliable experimental confirmation of this theory.

Solving the problems mentioned above will be greatly aided by the realization of the Chibis-AI microsatellite project (Space Research Institute, RAS), whose launch is planned for 2020. One of the main goals of the Chibis-AI satellite is to monitor both the high-energy processes using a gamma detector and the high-frequency radiation from atmospheric sources in the ultrashort wavelength band. Registration of high-energy radiation synchronously with radio band observations in combination with optical registration data from the GOES-R satellite (see Section 2) and the five-year projected service life of the microsatellite will make a significant contribution to the phenomenology and understanding of the mechanisms responsible for observable phenomena. We note that the upcoming launch of the TARANIS (tool for the analysis of radiation from lightning and sprites) microsatellite with similar scientific tasks and equipped with an optical detector will allow determining the spatial location of the radiation source and separating the spatial and temporal characteristics of the processes under investigation, which is impossible to realize when making observations using only one satellite.

This study was supported by the Russian Science Foundation grant 17-12-01439.

References

1. Christian H J et al. *J. Geophys. Res.* **108** 4005 (2003)
2. Rakov V A, Uman M A *Lightning*: *Physics and Effects* (New York: Cambridge Univ. Press, 2003)
3. Gurnett D A et al. *Geophys. Res. Lett.* **6** 511 (1979)
4. Warwick J W et al. *Science* **212** 239 (1981)
5. Zarka P, Pedersen B M *Nature* **323** 605 (1986)
6. Gurnett D A et al. *J. Geophys. Res.* **95** 20967 (1990)
7. Ksanfomaliti L V et al. *Sov. Astron. Lett.* **5** 122 (1979); *Pis'ma Astron. Zh.* **5** 229 (1979)
8. Raizer Yu P *Gas Discharge Physics* (Berlin: Springer, 1997); Translated from Russian: *Fizika Gazovogo Razryada* (Dolgoprudnyi: Intellekt, 2009)
9. Sadighi S et al. *J. Geophys. Res. Atmos.* **120** 3660 (2015)
10. Popov N A *J. Phys. D* **44** 285201 (2011)
11. Petersen D et al. *J. Geophys. Res.* **113** 17205 (2008)
12. Solomon R, Schroeder V, Baker M B *Q. J. R. Meteorol. Soc.* **127** 2683 (2001)
13. Loeb L B *J. Geophys. Res.* **71** 4711 (1966)
14. Griffiths R, Phelps C *J. Geophys. Res.* **81** 3671 (1976)
15. Phelps C T, Griffiths R F *J. Appl. Phys.* **47** 2929 (1976)
16. Gurevich A V, Milikh G M, Roussel-Dupre R *Phys. Lett. A* **165** 463 (1992)
17. Marshall T C, McCarthy M P, Rust W D *J. Geophys. Res.* **100** 7097 (1995)
18. Gurevich A V, Zybin K P, Roussel-Dupre R A *Phys. Lett. A* **254** 79 (1999)
19. Dwyer J R *Geophys. Res. Lett.* **32** L20808 (2005)
20. Dwyer J R, Babich L P *J. Geophys. Res.* **116** A09301 (2011)
21. Arabshahi S et al. *J. Geophys. Res. Space Phys.* **119** 479 (2014)
22. Liu N et al. *Phys. Rev. Lett.* **109** 025002 (2012)
23. Stalevich D D, Uchevatkina T S *Tr. Glav. Geofiz. Observ.* (405) 33 (1979)
24. Sin'kevich A A, Dovgalyuk Yu A *Radiophys. Quantum Electron.* **56** 818 (2014); *Izv. Vyssh. Uchebn. Zaved. Radiofiz.* **56** 908 (2013)
25. Lowke J J *J. Geophys. Res. Atmos.* **120** 3183 (2015)
26. Gurevich A V, Zybin K P *Phys. Today* **58** (5) 37 (2005)
27. Rison W et al. *Nature Commun.* **7** 10721 (2016)
28. Trakhtengerts V Yu *Dokl. Akad. Nauk SSSR* **308** 584 (1989)
29. Trakhtengerts V Yu, Iudin D I, in *Sprites, Elves and Intense Lightning Discharges* (NATO Science Series. Ser. II, Vol. 225, Eds M Füllekrug, E A Mareev, M J Rycroft) (Dordrecht: Springer, 2006) p. 341
30. Trakhtengertz V Yu, Mareev E A, Sorokin A E *Radiophys. Quantum Electron.* **40** 77 (1997); *Izv. Vyssh. Uchebn. Zaved. Radiofiz.* **40** 123 (1997)
31. Mareev E A, Sorokin A E, Trakhtengerts V Yu *Plasma Phys. Rep.* **25** 261 (1999); *Fiz. Plazmy* **25** (3) 123 (1999)
32. Iudin D I, Trakhtengerts V Y, Hayakawa M *Phys. Rev. E* **68** 016601 (2003)
33. Trakhtengerts V Y et al. *Phys. Plasmas* **9** 2762 (2002)
34. TrakhtengertsV Y et al. *Phys. Plasmas* **10** 3290 (2003)
35. Iudin D I, Davydenko S S *Radiophys. Quantum Electron.* **58** 477 (2015); *Izv. Vyssh. Uchebn. Zaved. Radiofiz.* **58** 530 (2015)
36. Davydenko S S, Iudin D I *Radiophys. Quantum Electron.* **59** 560 (2016); *Izv. Vyssh. Uchebn. Zaved. Radiofiz.* **59** 620 (2016)
37. Iudin D I *Radiophys. Quantum Electron.* **60** 374 (2017); *Izv. Vyssh. Uchebn. Zaved. Radiofiz.* **60** 418 (2017)
38. Landa P S, McClintock P V E *Phys. Rep.* **323** 1 (2000)
39. Bak P *How Nature Works*: *The Science of Self-Organized Criticality* (New York: Copernicus, 1996)
40. Wiesmann H J, Zeller H R *J. Appl. Phys.* **60** 1770 (1986)
41. Mansell E R et al. *J. Geophys. Res.* **107** 4075 (2002)
42. Iudin D I et al. *J. Geophys. Res. Atmos.* **122** 6416 (2017)
43. Hayakawa M, Iudin D I, Trakhtengerts V Yu *J. Atmos. Solar-Terr. Phys.* **70** 1660 (2008)
44. Iudin D I, Iudin F D, Hayakawa M *Radiophys. Quantum Electron.* **58** 173 (2015); *Izv. Vyssh. Uchebn. Zaved. Radiofiz.* **58** 187 (2015)
45. Zelenyi L M, Milovanov A V *Phys. Usp.* **47** 749 (2004); *Usp. Fiz. Nauk* **174** 809 (2004)
46. Albrecht R I et al., in *Proc. of the 14th Intern. Conf. on Atmospheric Electricity, Rio de Janeiro, Brazil, August 8 – 12, 2011*
47. Cecil D J, Buechler D E, Blakeslee R *Atmos. Res.* **135 – 136** 404 (2013)
48. Boccippio D J et al. *J. Atmos. Oceanic Technol.* **17** 441 (2000)
49. Goodman S J et al. *Atmos. Res.* **125 – 126** 34 (2013)
50. Holden D N, Munson C P, Devenport J C *Geophys. Res. Lett.* **22** 889 (1995)
51. Massey R S, Holden D N *Radio Sci.* **30** 1645 (1995)
52. Massey R S, Holden D N, Shao X M *Radio Sci.* **33** 1755 (1998)
53. Jacobson A R et al. *Radio Sci.* **34** 337 (1999)
54. Jacobson A R et al. *J. Geophys. Res.* **105** 15653 (2000)
55. Jacobson A R, Light T E L *J. Geophys. Res.* **108** 4266 (2003)
56. Smith D A et al. *Radio Sci.* **39** RS1010 (2004)
57. Jacobson A R *J. Geophys. Res.* **108** 4778 (2003)
58. Jacobson A R, Light T E L *Ann. Geophys.* **30** 389 (2012)
59. Zelenyi L M et al. *Cosmic Res.* **52** 87 (2014); *Kosmich. Issled.* **52** (2) 93 (2014)
60. Dolgonosov M S et al. *Adv. Space Res.* **56** 1177 (2015)
61. Fishman G J et al. *Science* **264** 1313 (1994)
62. Grefenstette B W et al. *J. Geophys. Res.* **114** A02314 (2009)
63. Briggs M S et al. *J. Geophys. Res. Space Phys.* **118** 3805 (2013)
64. Tavani M et al. (AGILE Team) *Phys. Rev. Lett.* **106** 018501 (2011)
65. Marisaldi M et al. *Geophys. Res. Lett.* **42** 9481 (2015)
66. Grove J E et al. *Am. Astron. Soc. Meeting Abstr.* **219** 149.13 (2012)
67. Kotov Yu D et al., in *The Coronas-F Space Mission* (Astrophysics and Space Science Library, Vol. 400, Ed. V Kuznetsov) (Berlin: Springer-Verlag, 2014) p. 175
68. Bogomolov V V et al. *Cosmic Res.* **55** 159 (2017); *Kosmich. Issled.* **55** (3) 169 (2017)
69. Roussel-Dupré R, Gurevich A V *J. Geophys. Res.* **101** 2297 (1996)
70. Horsthemke W, Lefever R *Noise-Induced Transitions* (Berlin: Springer, 1984)
71. Sancho J M, García-Ojalvo J *Lecture Notes Phys.* **557** 235 (2000)
72. Mikhailov A S, Uporov I V *Sov. Phys. Usp.* **27** 695 (1984); *Usp. Fiz. Nauk* **144** 79 (1984)
73. Dutton J *J. Phys. Chem. Ref. Data* **4** 577 (1975)
74. Popov N A *Plasma Phys. Rep.* **36** 812 (2010); *Fiz. Plazmy* **36** 867 (2010)
75. Hayakawa M, Iudin D I, Mareev E A, Trakhtengerts V Y *Phys. Plasmas* **14** 042902 (2007)
76. Rompe R, Weizel W *Z. Phys.* **122** 636 (1944)
77. Teunissen J, Ebert U *Comput. Phys. Commun.* (2018) https://doi.org/10.1016/j.cpc.2018.06.018; arXiv:1701.04329
78. Le Vine D M *J. Geophys. Res.* **85** 4091 (1980)
79. Cooray V et al. *Atmos. Res.* **149** 346 (2014)
80. Silva C L, Pasko V P *J. Geophys. Res. Atmos.* **120** 4989 (2015)
81. Nag A, Rakov V A *J. Geophys. Res.* **115** D20103 (2010)
82. Smith D A et al. *J. Geophys. Res.* **104** 4189 (1999)
83. Kostinskiy A Yu et al. *Geophys. Res. Lett.* **42** 8165 (2015)
84. Lazarus S M et al. *J. Geophys. Res. Atmos.* **120** 8469 (2015)
85. Wiens K C et al. *J. Geophys. Res.* **113** D05201 (2008)
86. Uman M A, McLain D K, Krider E P *Am. J. Phys.* **43** 33 (1975)
87. Jacobson A R, Holzworth R H, Shao X-M *Ann. Geophys.* **29** 1587 (2011)
88. Dwyer J R, Liu N, Rassoul H K *Geophys. Res. Lett.* **40** 4067 (2013)